Fully Relativistic Theory of the Ponderomotive Force in an Ultraintense Standing Wave

A. E. Kaplan* and A. L. Pokrovsky

Electrical and Computer Engineering Department, The Johns Hopkins University, Baltimore, Maryland 21218, USA

(Received 30 January 2005; revised manuscript received 20 April 2005; published 28 July 2005)

A relativistic field-gradient (ponderomotive) force in a laser standing wave ceases to exist in a familiar form; e.g., the adiabatic Hamiltonian is not separable into kinetic and potential energies for electrons moving in the antinode planes. We show that the force in the direction *across* the initial motion of an electron *reverses* its sign and makes the high-field areas attractive for electrons, opposite to a regular ponderomotive force. The reversal occurs at a relativistic-scale incident momentum, and represents the only effect known so far that pins down a distinct borderline between relativistic and nonrelativistic motion.

DOI: 10.1103/PhysRevLett.95.053601 PACS numbers: 42.50.Vk, 34.80.Qb, 42.65.Ky, 61.14.−x

A field-gradient (''ponderomotive'') force (PF) [1] is a cycle-averaged force on a charged particle in a spatially inhomogeneous electromagnetic (EM) field. A nonrelativistic PF attracts a particle regardless of its charge to low-intensity field areas and repels it from high-field areas. In a standard adiabatic approximation, it has a time-independent ''ponderomotive potential'' proportional to the field intensity; its full adiabatic energy has additive ''slow'' kinetic and potential components. The PF has many manifestations and applications, e.g., for laser trapping and cooling of atoms [2], high-field photoionization of atoms [3], and in the Kapitza-Dirac (KD) effect [4] in a standing EM wave. With the advent of laser technology, a PF acting on electrons enters the relativistic domain, if the laser field exceeds a scale $E_{\rm rel} = kmc^2/e$, whereby an electron is accelerated to a relativistic momentum within a half-cycle of the laser; here m is the rest mass of the electron, and $k = \omega/c$ and ω are the laser wave number and frequency. The relativistic PF is significant to the physics of electron beams in a strong laser field, plasmas and solids [5] irradiated by powerful lasers, etc. Such a PF in a *traveling wave* was explored in [6,7]. However, because of the high gradient between its nodes, the *standing wave* (SW) is one of the most interesting and fundamental configurations for a PF. The SW was also essential to the observation of relativistic hysteretic resonances [8] and nonlinear optics of a single electron [9]. Interesting work [10] on SWs concentrated on the transition to chaos and stochastic acceleration of electrons in free space using numerical simulations under the assumption that electrons are injected (e.g., due to photoionization) inside the laser beam.

In this Letter, we develop an analytical theory of a relativistic PF in a highly controllable and experimentally verifiable KD situation, whereby an electron with sufficiently high incident momentum is launched into a laser (L) beam from outside perpendicular to its axis; its results are also verified by numerical simulations. It allowed us to consider separately the PF along the SW planes and across them. We first found the adiabatic invariant and the characteristics of motion if an electron is launched in an antinode plane. For electrons launched along an arbitrary SW plane, the magnetic (M) laser field becomes a significant player and brings about a rich landscape of motion patterns. Our major discovery is that the PF in the direction *normal* to the incident momentum, $\vec{p}_0$, exhibits a dramatic sign reversal with a relativistic threshold: while remaining high-field repelling along $\vec{p}_0$, PF normal to $\vec{p}_0$ reverses into *high-field attractive force*, if $p_0 > mc$.

We consider two weakly focused Gaussian L beams counterpropagating and forming a SW in the y axis, an electron launched in the transverse x axis near their focal plane, and chose the electric ($\vec{E}$) field of a laser parallel to $\vec{p}_0$, and its spatial profile, $F(x)$ vanishing in the wings, $F(x) \to 0$ as $|x| \to \infty$. To concentrate on the significant features of the phenomenon, we assume ''slab'' 2D beams uniform in the z axis. Using normalized coordinates, $\xi = xk$, $\eta = yk$, $\zeta = zk$, time $\tau = \omega t$, momentum $\vec{\rho} = \vec{p}/mc$, relativistic factor $\gamma = \sqrt{1+\rho^2}$, and amplitude profile $f(\xi) = F/E_{\rm rel}$, we write $\vec{E}/E_{\rm rel} = \hat{e}_\xi \mathcal{E} f(\xi)$, with $\mathcal{E} = \cos\eta \sin\tau$ (the M field is ζ polarized), and the Lorentz equation as

$$\frac{d\vec{\rho}}{d\tau} = f(\xi)\left\{\hat{e}_\xi \mathcal{E} - \frac{\vec{\rho}\times\hat{e}_\zeta}{\gamma}\frac{d}{d\tau}\frac{\partial \mathcal{E}}{\partial \eta}\right\}, \qquad (1)$$

with $\rho_\xi = \gamma d\xi/d\tau$ and $\rho_\eta = \gamma d\eta/d\tau$.

We consider first an electron launched in an antinode plane, $\eta = n\pi$, where the E field has spatial maximum, and the M field *vanishes*. Allowing for thorough analytical treatment, which makes a good reference point, those planes are also strong attractors for relativistic trajectories; see below. Equation (1) is then reduced to

$$d\rho/d\tau = f(\xi)\sin\tau; \qquad d\xi/d\tau = \rho/\gamma. \qquad (2)$$

Choosing the sufficiently small field gradient, $df/d\xi \propto 1/\xi_L$, where ξ_L is the transverse size of L beam, and separating the electron motion $\xi(\tau)$ into slow (adiabatic) motion $\tilde{\xi}$ and ''fast'' oscillations $\delta\xi$, we will stipulate that the amplitude of the latter is small enough compared to that scale. Here the ''tilde'' indicates averaging over the oscillation cycle. One can show that $|\delta\xi| \le \pi/2$ for an arbitrary relativistic case. Indeed, the limiting speed of an

 © 2005 The American Physical Society

electron is $\beta = 1$, so that within a cycle the half-swing of electron is $\sim\pi/2$. For $f^2 \gg 1$ we can write $\beta \approx \mathrm{sign}(\rho)$, and the motion $\xi(\tau)$ assumes a saw-teeth shape (Fig. 1). [All the figures here were obtained by numerical solution of (1) or (2) in the Gaussian-like profile $f(\xi)$.] The condition of laser ξ-profile smoothness is

$$\xi_L \gg \xi_{\mathrm{osc}} \equiv \min(\pi/2, f_{pk}) \quad \text{or} \quad \mu_\xi \equiv \xi_{\mathrm{osc}}/\xi_L \ll 1, \tag{3}$$

where f_{pk} is the peak magnitude of $f(\xi)$ and μ_ξ is a small parameter [11]. Note that the fast oscillations of momentum and energy *may be large*. Writing $f(\xi) = f(\tilde{\xi}) + (df/d\tilde{\xi})\delta\xi + O(\mu_\xi^2)$ and the Fourier series for $\delta\xi$, we have from (2) that, to the terms $O(\mu_\xi)$,

$$\xi \approx \tilde{\xi} + \xi_1(\tilde{\xi})\sin\tau; \qquad \rho \approx \tilde{\rho} - f(\tilde{\xi})\cos\tau. \tag{4}$$

Adiabatic equations for slow motion alone are then as

$$\frac{d\tilde{\rho}}{d\tau} = \frac{1}{2}\frac{df(\tilde{\xi})}{d\tilde{\xi}}\xi_1[\tilde{\rho}, f(\tilde{\xi})]; \qquad \frac{d\tilde{\xi}}{d\tau} = \tilde{\beta}[\tilde{\rho}, f(\tilde{\xi})], \tag{5}$$

with $2\pi\tilde{\beta} = \int_0^{2\pi}(\rho/\gamma)d\tau$ and $\pi\xi_1 = \int_0^{2\pi}(\rho/\gamma)\cos\tau d\tau$, where ρ is as in (4), and $\gamma = \sqrt{1+\rho^2}$. Let us introduce $H(\tilde{\rho}, \tilde{\xi}) \equiv \tilde{\gamma} = (2\pi)^{-1}\int_0^{2\pi}\gamma(\tilde{\rho}, \tilde{\xi}, \tau)d\tau$. (Note that in general $H = \tilde{\gamma} \neq \sqrt{1+\tilde{\rho}^2}$ and $\tilde{\beta} \neq \tilde{\rho}/\tilde{\gamma}$.) It is then readily verified that (5) can now be written in the canonical Hamiltonian form as

$$\frac{d\tilde{\rho}}{d\tau} = -\frac{\partial[H(\tilde{\rho}, \tilde{\xi})]}{\partial\tilde{\xi}}; \qquad \frac{d\tilde{\xi}}{d\tau} = \frac{\partial[H(\tilde{\rho}, \tilde{\xi})]}{\partial\tilde{\rho}}, \tag{6}$$

from which it transpires that $H(\tilde{\rho}, \tilde{\xi})$ is the (adiabatic) *Hamiltonian*, and thus is to be conserved during the motion. Indeed, using (6) one can show that $dH/d\tau = 0$, so that H is *the invariant of motion*: $H = \mathrm{inv} = \gamma_0$, where γ_0 is the relativistic factor of incident electron. The same result is obtained by assuming an arbitrary phase ϕ of the laser field, i.e., by replacing τ in (2) by $\tau + \phi$. For an *incoherent* electron beam with electrons arriving randomly, time averaging can be replaced by averaging over the ensemble of all the phases $0 \leq \phi < 2\pi$; by designating it with angular brackets, we see that the system is *ergodic*: $\langle\xi\rangle = \tilde{\xi}$, $\langle\rho\rangle = \tilde{\rho}$, $\langle\beta\rangle = \tilde{\beta}$, and

$$H(\tilde{\rho}, \tilde{\xi}) = \tilde{\gamma} = \langle\gamma\rangle = \mathrm{inv} = \gamma_0. \tag{7}$$

This is a conservation of a full (adiabatic) relativistic energy. Elegantly simple, Eq. (7) is yet not too obvious, for $\tilde{\gamma}$ cannot be separated into kinetic and potential energies except for the nonrelativistic case; see below. The averaging in $\tilde{\gamma}$ over huge nonlinear oscillations of momentum in fact makes it amazing that (7) holds.

In nonrelativistic case ($\rho^2, f^2 \ll 1$), one has, as expected, $\tilde{\rho}^2/2 + U(\tilde{\xi}) = \mathrm{inv} = \tilde{\rho}_0^2/2$, where $\tilde{\rho}^2/2$ is slow kinetic energy, and $U(\tilde{\xi}) = f^2(\tilde{\xi})/4$ is an effective potential: the only case when they can be separated. However, in a *strongly relativistic field*, $f(\xi)^2 \gg 1$, whereby during most of the time $\gamma \approx |\rho|$, (7) yields

$$\tilde{\rho}\sin^{-1}[\tilde{\rho}/f(\tilde{\xi})] + \sqrt{f^2(\tilde{\xi}) - \tilde{\rho}^2} = \mathrm{inv} = \pi\rho_0/2 \tag{8}$$

if $\tilde{\rho}^2/f^2 \leq 1$, and $\tilde{\rho}^2 \approx \rho_0^2$ otherwise; no specific terms can be assigned here to either kinetic or potential energies.

A turning point, $\tilde{\xi}_{\mathrm{trn}}$, at which the electron slow trajectory comes to a complete stop, i.e., $\tilde{\rho} = 0$, is determined by $H(0, \tilde{\xi}_{\mathrm{trn}}) = \gamma_0$. A threshold incident momentum ρ_{thr}, marking the switching from full reflection ($\rho_{\mathrm{out}} = -\rho_0$) to full transmission ($\rho_{\mathrm{out}} = \rho_0$), corresponds to $\tilde{\xi}_{\mathrm{trn}} = f_{\mathrm{pk}}$. Our calculations show that ρ_{thr} vs f_{pk} is an almost linear function; writing $\rho_{\mathrm{thr}} = af_{\mathrm{pk}}$, we have $a = 1/\sqrt{2}$ for $f_{\mathrm{pk}}^2 \ll 1$ and $a = 2/\pi$ for $f_{\mathrm{pk}}^2 \gg 1$.

We will now move into the planes with a nonvanishing M field. In nonrelativistic case, the second (M field) term on the right-hand side of (1) is small since $\rho \ll 1$. In linearly polarized *traveling* wave for $\rho \gg 1$ [6] it results in "8"-like trajectories. A SW opens a whole new can of worms: oscillation "channeling" of electrons and reversion of attraction areas, "sneaky" transmission modes, a huge KD effect in transmission and *reflection*, etc.

For the motion normal to the SW planes, the fundamental fact that *rules out* general adiabatic theory is that at $\gamma \gg 1$ the full swing of fast oscillations across the SW planes may reach $\lambda/2$, which is the spacing between adjacent SW planes. This disallows the assumption that the η-inhomogeneity scale can *always* be small, since $(\mu_\eta)_{\max} = (\eta_{\mathrm{osc}})_{\max}/\pi = 1$ [compare with (3)]. Numerical simulations [10] in most of the cases exhibit chaos. Here we are interested in well-controlled electron motion that would enable us to predict and use new physical effects and determine their characteristics and areas of existence, in particular, the accessibility and stability domains of the various modes (e.g., antinode modes).

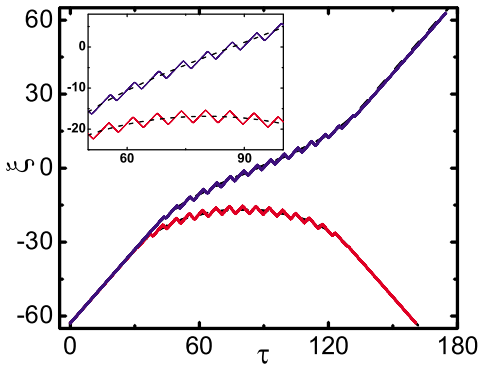

FIG. 1 (color online). Typical motions of electrons passing through (upper curve) and reflected from (lower curve) the antinode of laser SW. Here $\rho_0 = 11$ and 8, respectively, with the threshold $\rho_{\mathrm{thr}} \approx 9.59$. The laser profile is taken as $f(\xi) = f_{\mathrm{pk}}\cos^2(\xi/\xi_L)$ at $|\xi| < \pi\xi_L/2$ and $f(\xi) = 0$ otherwise, with $f_{\mathrm{pk}} = 15$ and $\xi_L = 40$. Solid lines, the full motion ξ; dashed lines, time-averaged $\tilde{\xi}$. The inset depicts an enlarged center region of the main plot.

If the initial electron momentum dominates the laser field, $\mu_L = f_{\rm pk}/\rho_0 \ll 1$, the motion is adiabatic and can be well analyzed; this condition does not preclude relativistic ρ_0 and $f_{\rm pk}$. Assuming again slow + fast motion, $(\delta\xi)_{\max} \equiv \mu_\xi = O(\xi_L^{-1}) \ll 1$, and $(\delta\eta)_{\max} = \mu_L \ll 1$, where $\delta\xi$ and $\delta\eta$ are fast ξ and η oscillations, we obtain that to $O(\max(\mu_L, \mu_\xi))$, $\rho_\xi \approx \rho_0$, $\xi = \tilde{\xi} \approx \beta_0\tau$, and $\eta = \tilde{\eta} + \delta\eta$. Writing $\rho_\eta = \tilde{\rho}_\eta + \delta\rho_\eta$, using this in (1) and retaining the terms of lowest order in μ_ξ and μ_L, we find that $\delta\eta = f(\tilde{\xi})\tilde{\rho}_\xi\tilde{\gamma}^{-2}\cos\tau\sin\tilde{\eta}$ and $\delta\rho_\eta = -f(\tilde{\xi})\tilde{\rho}_\xi\tilde{\gamma}^{-1}\sin\tau\sin\tilde{\eta}$, and the dynamics of slow variables is governed by beautifully simple and revealing equations:

$$\frac{d^2\tilde{\eta}}{d\tau^2} + f^2(\beta_0\tau)\frac{\rho_0^2 - 1}{4\gamma_0^4}\sin(2\tilde{\eta}) = 0, \quad \tilde{\rho}_\eta = \gamma_0\frac{d\tilde{\eta}}{d\tau}; \quad (9)$$

i.e., the η oscillations are pendulumlike. Their small-oscillation slowly varying frequency is as

$$\Omega_\eta(\tau) = f(\beta_0\tau)\sqrt{|\rho_0^2 - 1|}/(\sqrt{2}\gamma_0^2), \quad (10)$$

and it peaks out at the middle of the L beam, where $f = f_{\rm pk}$. The equilibrium points of (9) are $\eta = \pm n\pi/2$; each stable point (focus) is alternated by an unstable point (saddle). The most remarkable feature here is that at a certain reversal point, $\rho_0^2 = 1$, slow oscillations vanish, while the stable and unstable points of (9) switch their positions. At $\rho_0^2 < 1$, the stable points are $\eta = (n + 1/2)\pi$; hence the planes of attraction for the trajectories are the nodes [see Fig. 2(a′)], i.e., the planes of maximum M field (and zero E field) (the points $\eta = n\pi$ are unstable). Slow oscillating solid lines for $\tilde{\rho}_\eta(\tau)$ in Figs. 2(a) and 2(b), obtained directly from numerical solution of (9), coincide within the line thickness with the cycle averaging of the full motion. However, in the relativistic area, $\rho_0^2 > 1$, the points $\eta = n\pi$ become stable [Fig. 2(b)] and the antinodes, considered in detail in the first part of this Letter, become the plane of attraction, whereas $\eta = (n + 1/2)\pi$ become unstable. At $\rho_0^2 = 1$, we have $\Omega_\eta = 0$ [Figs. 2(c) and 2(c′)]. In fact, it is the only effect known to us that pins down a clear borderline between "relativistic" and "nonrelativistic" motions. This borderline corresponds to $\gamma_0 = \sqrt{2}$, or ~212 keV electron kinetic energy, which can readily be accessed with an electron microscope. In the nonrelativistic limit, Eq. (9) reduces to a regular η-gradient-force equation with $\rho_0 \ll 1$ and $\gamma_0 \approx 1$, and nodes $\tilde{\eta} = (n + 1/2)\pi$ being stable points.

The reversal effect here can be explained this way. The PF, which is normal to both $\vec{E}$ and $\vec{p}_0$, is induced by the second, "magnetic" term on right-hand side of (1), proportional to γ^{-1}. Fast oscillations of γ (as, e.g., in [9]) create a relativistic force counteracting to the "regular" PF and becoming dominant at $\rho_0 > 1$; at $\rho_0 = 1$, these two nearly cancel each other. [In the 1D case, Eq. (2), the magnetic term is absent.]

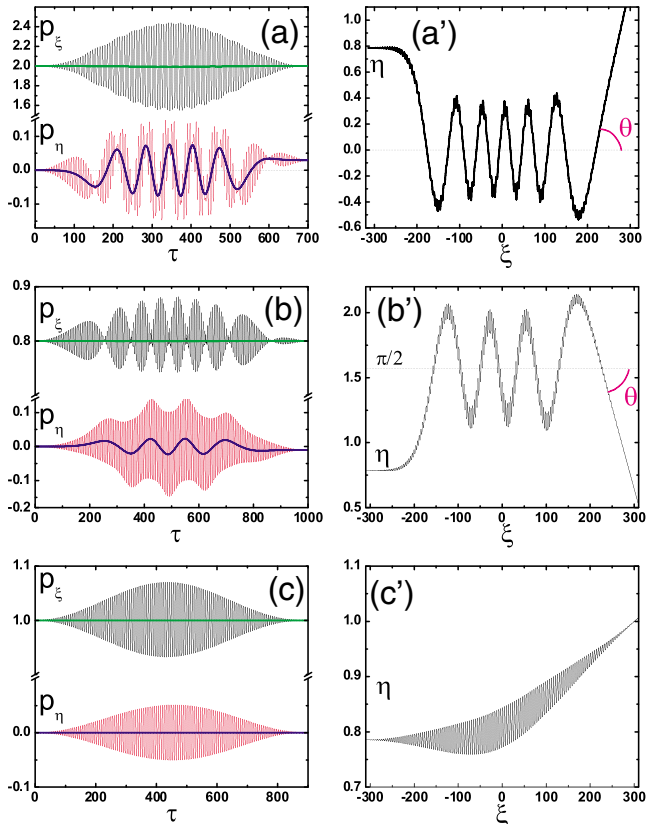

FIG. 2 (color online). Momenta [(a)–(c)] and trajectories [(a′)–(c′)] of electron normally incident on the L beam at $\eta_0 = \pi/4$ with initial momentum p_0 above [(a),(a′): $\rho_0 = 2$, $f_{\rm pk} = 0.45$], below [(b),(b′): $\rho_0 = 0.8$, $f_{\rm pk} = 0.2$], and at switching threshold [(c),(c′): $\rho_0 = 1$, $f_{\rm pk} = 0.1$]. At $\tau = 0$, $\xi = -\pi\xi_L/2$ and $\xi_L = 200$.

Equation (9) also describes the trajectory $\tilde{\eta}(\tilde{\xi})$ if τ is replaced with $\tilde{\xi}/\beta_0$, so that $d^2\tilde{\eta}/d\tilde{\xi}^2 + [f^2(\tilde{\xi}) \times (\rho_0^2 - 1)/(2\rho_0\gamma_0)^2]\sin(2\tilde{\eta}) = 0$. If an electron makes a few η oscillations, i.e., if $(\Omega_\eta)_{\rm pk}\xi_L/\beta_0 \gg 1$, the small η oscillations with the launching point $\eta = \eta_0$, can be obtained from (9) via WKB approximation as $\eta(\tau) \propto (\eta_0 - \eta_{\rm st})\sqrt{f_{\rm pk}/f(\tau\beta_0)}\sin[\Phi(\tau)]$, where $\Phi(\tau) = \int_{-\infty}^{\tau}\Omega_\eta(t)dt \gg 2\pi$ and $\eta_{\rm st}$ is a stable point nearest to η_0; it explains why the slow η oscillations are pinched down at the peak field. These oscillations can be observed via the E beam EM radiation with the low frequency spectrum that has a cutoff frequency $\Omega_{\rm cut} = f_{\rm pk}\sqrt{|\rho_0^2 - 1|/2}/\gamma_0^2$, as well as via modulation of the scattered laser with frequencies $\omega_{\rm scat} = \omega_L \pm \Omega_\eta$, i.e., self-scattering of laser at electrons in a quasiresonant SW system. The highest possible $\Omega_{\rm cut}$ for a given $f_{\rm pk}$ corresponds to $\rho_0 = \sqrt{3}$, at which $(\Omega_{\rm cut})_{\max} = f_{\rm pk}/4$. Because of the η oscillations, when an electron approaches the far outer edge of the L beam, it can be angularly deflected due to a "slingshot" effect, thus causing a superstrong relativistic KD effect. The highest pos-

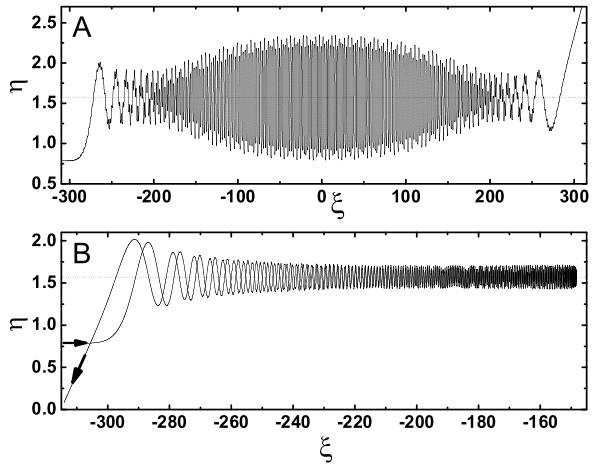

FIG. 3. Transmission (a) and reflection (b) trajectories of electron normally incident on the L beam ($f_{\rm pk} = 2$, $\xi_L = 200$) at $\eta_0 = \pi/4$; $\rho_0 = 0.325$ (a) and 0.06 (b).

sible angle of deflection, $\theta_{\max} \sim (\tilde{\rho}_\eta)_{\max}/\rho_0$, is estimated as

$$\theta_{\max} \sim (\pi/2^{3/2})(f_{\rm pk}/\rho_0)\sqrt{|\rho_0^2 - 1|/\gamma_0} \qquad (11)$$

or, if $\rho_0^2 \gg 1$, $\theta_{\max} \sim (\pi/2^{3/2}) f_{\rm pk}/\rho_0$; e.g., for $\rho_0 = 2$ and $f_{\rm pk} = 1/\sqrt{2}$, we have $\theta_{\max} \sim \pi/8$, a huge effect. This KD deflection for $\rho_0^2 \neq 1$ is seen in Figs. 2(a) and 2(a′) and Figs. 2(b) and 2(b′) for $\tilde{\rho}_\eta$ and especially for $\tilde{\eta}$; it also exists even for $\rho_0^2 = 1$ [Fig. 2(c′)], but is too small to show up in $\tilde{\rho}_\eta$ [Fig. 2(c)].

Sufficient conditions to prevent the system from sliding into instability and chaos are that the incident momentum is strong enough compared to the E field, $\rho_0^2 \gg f_{\rm pk}^2$, or the L beam size, $2\xi_L$, is sufficiently short. In fact, strong chaos in SW in [10] was apparently facilitated by an electron being born inside the L beam and having low initial momentum, and the L beam size being very large or infinite. For $\rho_0 > 1$, the most ''permissive'' middle entrance point $\eta_0 = \pi/4$, and sufficiently long run $\xi_L = 200$ (50λ waist), we found that the stability area for $\rho_0 > 1$ is determined by a simple formula, $\rho_0/f_{\rm pk} > \text{const} \approx 2$.

The areas of parameters $f_{\rm pk}$, ρ_0, and η_0, where the system is still stable, exist even if $f_{\rm pk}^2 \gg \rho_0^2$, albeit they are relatively narrow. Of interest here are reflection modes; even if $f_{\rm pk}^2 \gg 1$, but ρ_0 is sufficiently small (typically <0.07), the slow ξ motion may came to a complete stop far before it reaches the point where f peaks out [Fig. 3(b)]. For $f_{\rm pk} < 2.3$, there are still areas of ρ_0 and η_0, where electrons with relatively low ρ_0 are still able to ''sneak through'' [Fig. 3(a)].

In conclusion, our relativistic analytical theory of the electron motion in a standing wave of an ultrapowerful laser showed that the ponderomotive force, as it is known in the nonrelativistic case, gets transformed into a much richer set of spatial interactions. Our major result is that the PF normal to the incident momentum switches its sign as the momentum exceeds relativistic scale, which makes high-intensity areas (antinodes) attractive instead of the expected low-intensity areas (nodes). We also found an adiabatic invariant for antinode modes, sneaky modes in the nodes, and a large Kapitza-Dirac effect. Our numerical simulations confirmed the analytical results.

This work is supported by AFOSR.

*Electronic address: sasha@striky.ece.jhu.edu

[1] H. A. H. Boot and R. B. R.-S. Harvie, Nature (London) **180**, 1187 (1957); A. V. Gaponov and M. A. Miller, Sov. Phys. JETP **7**, 168 (1958); T. W. B. Kibble, Phys. Rev. Lett. **16**, 1054 (1966); F. A. Hopf *et al.*, *ibid.* **37**, 1342 (1976).

[2] A. Ashkin, Phys. Rev. Lett. **24**, 156 (1970); T. W. Hänsch and A. L. Schawlow, Opt. Commun. **13**, 68 (1975); for a review, see, e.g., *Laser Manipulation of Atoms and Ions*, edited by E. Arimondo, W. D. Phillips, and S. Strumina (North-Holland, Amsterdam, 1992); G. Grynberg and C. Robilliard, Phys. Rep. **355**, 335 (2001).

[3] R. R. Freeman *et al.*, Phys. Rev. Lett. **59**, 1092 (1987); E. Wells, I. Ben-Itzhak, and R. R. Jones, *ibid.* **93**, 023001 (2004).

[4] P. L. Kapitza and P. A. M. Dirac, Proc. Cambridge Philos. Soc. **29**, 297 (1933); M. V. Fedorov, Opt. Commun. **12**, 205 (1974); P. H. Bucksbaum, D. W. Schumacher, and M. Bashkansky, Phys. Rev. Lett. **61**, 1182 (1988); D. L. Frelmund, K. Aflatoonl, and H. Batelaan, Nature (London) **413**, 142 (2001).

[5] C. Gahn *et al.*, Phys. Rev. Lett. **83**, 4772 (1999); J. Faure *et al.*, Nature (London) **431**, 541 (2004).

[6] E. S. Sarachik and G. T. Shappert, Phys. Rev. D **1**, 2738 (1970).

[7] J. N. Bardsley, B. M. Penetrante, and M. H. Mittleman, Phys. Rev. A **40**, 3823 (1989); F. V. Hartemann *et al.*, Phys. Rev. E **51**, 4833 (1995); Y. I. Salamin and F. H. M. Faisal, Phys. Rev. A **55**, 3678 (1997); J. L. Chaloupka and D. D. Meyerhofer, Phys. Rev. Lett. **83**, 4538 (1999).

[8] A. E. Kaplan, Phys. Rev. Lett. **48**, 138 (1982); G. Gabrielse, H. Dehmelt, and W. Kells, *ibid.* **54**, 537 (1985).

[9] A. E. Kaplan, Phys. Rev. Lett. **56**, 456 (1986); A. E. Kaplan and Y. J. Ding, IEEE J. Quantum Electron. **24**, 1470 (1988); C. S. Weimer, F. L. Moore, and D. J. Wineland, Phys. Rev. Lett. **70**, 2553 (1993); E. Yablonovitch, N. Bloembergen, and J. J. Wynne, Phys. Rev. B **3**, 2060 (1971).

[10] D. Bauer, P. Mulser, and W.-H. Steeb, Phys. Rev. Lett. **75**, 4622 (1995); Z.-M. Sheng *et al.*, Phys. Rev. E **69**, 016407 (2004).

[11] The effects here are strongly classical; typically, the photon number $N_{\rm ph}$ per electron per cycle far exceeds $mc^2/\hbar\omega = O(10^6)$, and quantum dispersion is $(N_{\rm ph})^{-1/2} \ll \mu_\xi$.